Available online at www.sciencedirect.com
SCIENCE DIRECT
Tetrahedron 62 (2006) 3619–3628
Tetrahedron

Homohelicity induction of propylene-linked zinc bilinone dimers by complexation with chiral amine and α-amino esters. Preorganization of structurally coupled homohelical subunits

Katsushi Hamakubo,[a] Shigeyuki Yagi,[a,*] Hiroyuki Nakazumi,[a] Tadashi Mizutani[b] and Susumu Kitagawa[c]

[a]*Department of Applied Chemistry, Graduate School of Engineering, Osaka Prefecture University, Gakuen-cho, Sakai, Osaka 599-8531, Japan*
[b]*Department of Molecular Science and Technology, Faculty of Engineering, Doshisha University, Kyotanabe, Kyoto 610-0321, Japan*
[c]*Department of Synthetic Chemistry and Biological Chemistry, Graduate School of Engineering, Kyoto University, Nishikyo-ku, Kyoto 615-8530, Japan*

Received 9 December 2005; revised 24 January 2006; accepted 25 January 2006

Available online 28 February 2006

Abstract—Homohelicity induction of a series of propylene-linked zinc bilinone (ZnBL; linear tetrapyrrople-zinc(II) complex) dimers upon complexation with chiral amine and α-amino esters was investigated. Introduction of substituents such as dimethyl and diisobutyl to the central carbon of the propylene spacer gave rise to stabilization of the homohelical (*PP* and *MM*) conformers rather than the heterohelical (*PM*) conformer. As bulkiness of the substituent increased, stability of the homohelical conformers was raised. The preorganization of the homohelical structures led to significantly amplified homohelicity induction upon complexation with chiral amine and α-amino esters.

1. Introduction

Construction of multitopic receptors possessing structurally coupled subunits is a key matter to obtain amplified functions induced by chemical stimuli. In biological systems, allosteric proteins enhance or suppress their activities via cooperative motion of coupled subunits.[1] Hemoglobin, which consists of four subunits, is one of typical examples, where the first binding of an O_2 molecule to one of four subunits gives rise to its conformational change to induce the increasing O_2-affinity of the other subunits.[2] In artificial systems, a set of cooperatively operating guest-binding subunits is one of good candidates for construction of signal transmission/amplification systems for external stimuli, and therefore, is potentially applicable to molecular sensory systems and other signal transmitting devices.[3] Great efforts have so far been poured to investigation of allosteric host molecules possessing structurally coupled heterotopic and homotopic binding-sites.[4,5] However, few examples of host molecules that amplify structural information of chiral guests to provide integrated spectroscopic signals have been reported.[6–9] In order to develop a signal transmission/amplification system for chiral molecules, here we report homohelicity induction of zinc bilinone (ZnBL) dimers triggered by complexation with chiral amine and α-amino esters.

As shown in Figure 1, ZnBL is a linear tetrapyrrole zinc(II) complex and possesses a helical structure due to steric

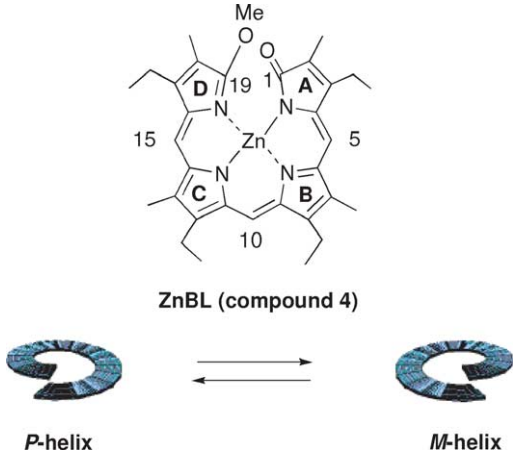

Figure 1. The helical structure and equilibria of zinc bilinone (ZnBL, compound **4**). The labels of A–D represent the custom naming for pyrrole rings.

Keywords: Zinc bilinone; Substituent effect; Homohelicity induction; Preorganization.
* Corresponding author. Tel.: +81 72 2549324; fax: +81 72 2549913; e-mail: yagi@chem.osakafu-u.ac.jp

0040–4020/$ - see front matter © 2006 Elsevier Ltd. All rights reserved.
doi:10.1016/j.tet.2006.01.089

repulsion between 1- and 19-oxygen atoms as well as a template effect of the central zinc ion. The helix inversion between the right-handed (*P*) and left-handed (*M*) helical conformers easily occurs due to the low energetic barrier. We previously reported that coordination of a chiral amine or a chiral α-amino ester to the zinc center induced preferred helicity of ZnBL (e.g., the compound **4** in Fig. 1).[10] Especially, the induced helicity showed good correspondence with chirality of the amino esters; *P*-helix for D-amino esters and *M*-helix for the L-isomers. The helicity excess (h.e.), that is, the diastereomeric excess of the ZnBL–guest complex with preferred helicity, depended on the structures of the chiral guests. The helicity induction process was conveniently monitored by ^{1}H NMR as well as circular dichroism (CD) spectroscopy.

In the case of ZnBL dimers, equilibria among the *PP*-, *PM*-, and *MM*-conformers exist as shown in Figure 2. If the two ZnBL subunits do not affect each other, each ZnBL subunit should behave just as a monomer upon complexation with a chiral guest. On the other hand, structural perturbation by steric interaction between the ZnBL subunits should break the statistical balance of the equilibria among three conformers, and the thermodynamically preferred conformer should be predominantly formed. Indeed, in the ethylene-linked ZnBL dimer previously reported, homohelicity induction efficiently occurred upon complexation with chiral α-amino esters, and the complexation-induced CD signal normalized by a molar concentration of the ZnBL subunit was enhanced compared with that in the ZnBL monomer.[8] On the other hand, the propylene-linked ZnBL dimer exhibited negative cooperativity, that is, heterohelicity enrichment, upon complexation with the chiral guests, indicating that the increase in flexibility of the spacer is unfavorable for cooperative motion of the ZnBL subunits.

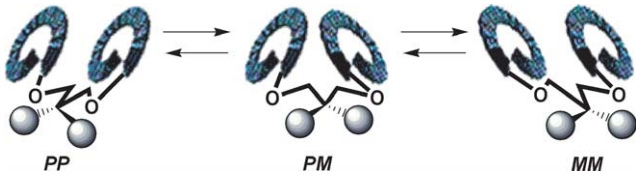

Figure 2. Illustration of equilibria in the ZnBL dimer system. Here the propylene-linked dimer is illustrated.

In the present study, we show preorganization of the *PP* and *MM* homohelicity conformers of the propylene-linked ZnBL dimer, where introduction of bulky substituents onto the central carbon of the spacer leads to stabilization of the homohelical (*PP* and *MM*) conformers rather than the heterohelical one (*PM*). We also report that the preorganization of the homohelical conformers leads to significantly enhanced homohelicity induction upon complexation with the chiral guests.

2. Results and discussion

2.1. Preparation of the propylene-linked ZnBL dimers

ZnBL dimers **1**–**3** were employed in this study. In **1**, two ZnBL moieties are linked by a propylene spacer. On the other hand, in **2** and **3**, dimethyl and diisobutyl substituents are introduced onto the central carbon atom in the propylene spacer, respectively. Preparation of **1** was reported previously.[8] Preparation of the dimers **2** and **3** was carried out in a modified way of preparation of **1**, as shown in Scheme 1. The ring-opening reaction of 2 equiv of

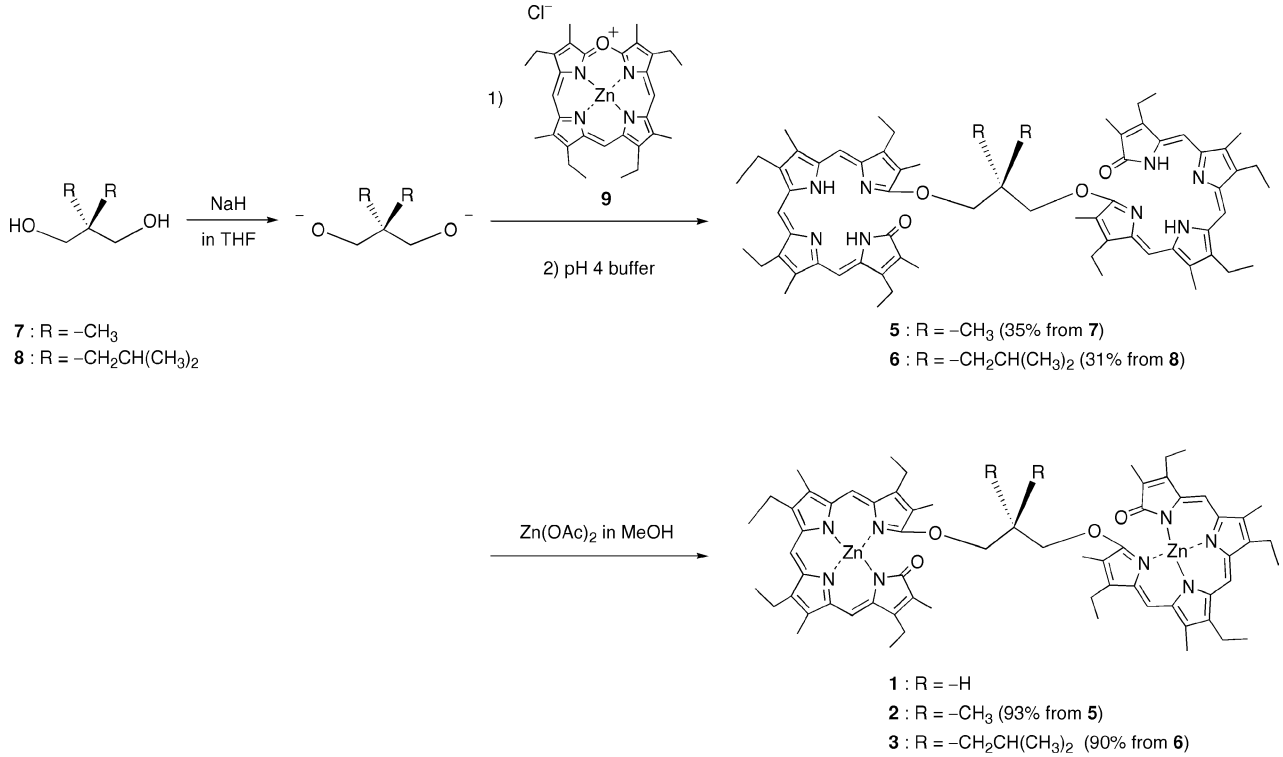

Scheme 1. Synthesis of ZnBL dimers.

(5-oxoniaporphyrinato)zinc(II) chloride **9** with 1 equiv of the dialkoxides of **7** and **8** followed by treatment with a buffer solution (pH 4) yielded the free-base bilinone dimers **5** and **6** in 35 and 31% yields, respectively.[11,12] Insertion of zinc(II) ions to **5** and **6** afforded the ZnBL dimers **2** and **3** in 93 and 90% yields, respectively. The ZnBL dimers were so sensitive to usual ways of purification such as silica or alumina column chromatography and recrystallization in a hot solvent as to give rise to demetallation of zinc(II) ions. Thus, the corresponding free-base bilinone dimers were thoroughly purified by silica gel column chromatography followed by gel permeation chromatography and reprecipitation, and then the ZnBL dimers were obtained just by zinc insertion to the free-base dimers. These dimers were characterized by ^{1}H NMR, IR and FAB MS spectra as well as elemental analyses. The assignment of the ^{1}H NMR signals of **2** and **3** was achieved using ROESY and HMBC techniques.

2.2. Stabilization of the homohelical conformers by introduction of bulky substituents on the spacer

In Figure 3 are shown the expanded region of the ^{1}H NMR spectra of **1**–**3** in $CDCl_3$ at 223 K. For each dimer, two sets of signals were observed with different integral ratios, which were assigned to the homohelical (*PP* and *MM*) and heterohelical (*PM*) conformers. As discussed later, the three conformers are distinguishable from one another upon complexation with chiral guests. In the complexed homohelical conformers ($PP\cdot 2G^*$ and $MM\cdot 2G^*$; G^*, chiral guest), two ZnBL subunits are magnetically equivalent. In addition, the $PP\cdot 2G^*$ and $MM\cdot 2G^*$ complexes are diasteromeric to each other, and their ^{1}H signals are observed independently with different integral ratios. On the other hand, in the complexed heterohelical conformer ($PM\cdot 2G^*$), the two subunits are magnetically unequivalent. Thus, the distribution of the three conformers can be determined. The ratio of *PP*:*PM*:*MM* for **1** was 22:56:22, showing approximation to statistical distribution (25:50:25). This indicated that two ZnBL subunits were likely to behave independently. On the other hand, the ratios of *PP*:*PM*:*MM* for **2** and **3** are 33:35:33 and 46:8:46, respectively. Obviously, the increase in steric hindrance on the spacer led to stabilization of the homohelical conformers. Therefore, the bulkiness of the substituents on the propylene spacer plays an essential role in positive cooperativity of formation of the homohelical conformers.

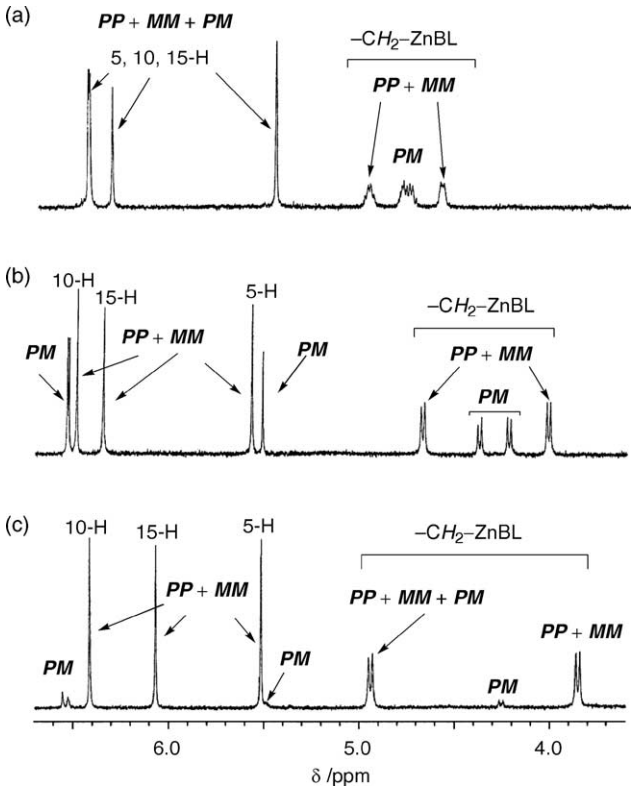

Figure 3. The expanded region of the ^{1}H NMR spectra of (a) **1**, (b) **2**, and (c) **3** in $CDCl_3$ at 223 K. The concentration of each dimer is 1.07–1.09 mM.

Interesting is that the cooperativity was enhanced by complexation of an achiral amine with each ZnBL subunit in the dimers. Upon addition of increasing amounts of benzylamine to solutions of **1**–**3**, all signals exhibited chemical shift changes accompanied by saturation behaviors (Fig. 4), and finally, the ratios of *PP*:*PM*:*MM* for **1**, **2** and **3** reached 15:70:15, 39:22:39 and 49:2:49, respectively. Upon complexation with benzylamine, the formation of the heterohelical conformer was facilitated in **1**, whereas the homohelical conformers were enriched in **2** and **3**. That is, coordination of the ligand to each zinc center enhanced the cooperativity between the two ZnBL subunits.

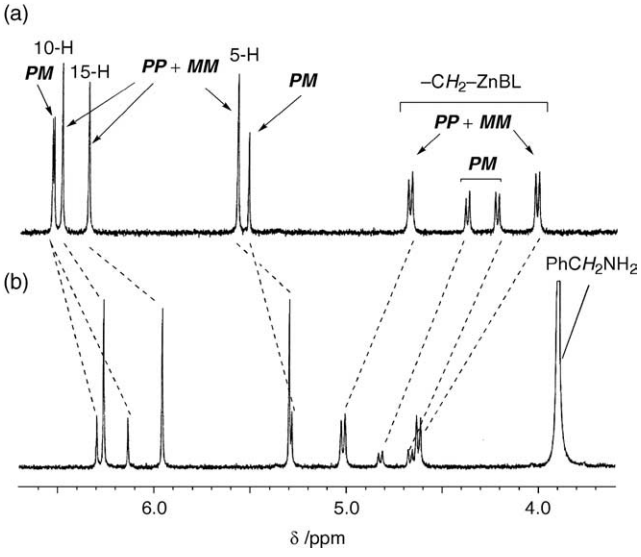

Figure 4. The expanded region of the ^{1}H NMR spectra of **2** in $CDCl_3$ at 223 K; (a) **2** (1.09 mM), (b) **2** (1.09 mM) and benzylamine (6.53 mM).

2.3. Molecular modeling study on stability of the homohelical conformers

Molecular modeling studies based on molecular mechanics and molecular orbital calculations afford valuable information on the geometries and energetics of supramolecules.[13] Most of the molecular orbital studies, however, are concerned with hydrogen bonding,[14–15] and less attention has been paid to the non-polar interactions such as attractive van der Waals forces. This is due to the fact that much more elaborate calculations, for instance the MP2 theory, are

needed to evaluate London's dispersion forces, and such calculations are limited to small molecular systems, such as a N_2–CO_2 complex[16] and a fucose–benzene complex.[17] We performed semi-empirical calculations of our ZnBL dimers in order to evaluate the importance of steric repulsive forces in the conformational equilibria. In the previous study, an important role of steric bulk of the guest molecules was revealed in binding energetics to zinc porphyrins.[18]

In order to obtain structural details about stability of the homohelical conformers, molecular modeling studies using grid search calculations were examined for the *PP* conformers of **1**–**3**. Particular attention was paid to the role of the steric bulk introduced to the spacer in the restriction of conformation of the dimers. As shown in Figure 5a, the bond rotation around O19–C1 defined by the dihedral angle θ of the C1–C2 and O19–C19 bonds were examined, where θ_0 represents the value of θ of the initial structure.[19] The grid search calculations were carried out for the 12 angles at 30° intervals, and the geometry was fully optimized except for θ by molecular orbital calculations at the MOPAC PM3 level.[20] In Figure 5b are shown plots of the changes in the enthalpy of formation ΔH_{PP} for **1**–**3** against the angle $\theta-\theta_0$. Obviously, no significant differences in ΔH_{PP} at any $\theta-\theta_0$ were observed in **1**. On the other hand, introduction of dimethyl or diisobutyl groups to the spacer brought about restriction of the preferred $\theta-\theta_0$ affording stable conformers, and the tendency was more remarkable in **3** than in **2**.

Comparison of the conformational energies of homohelical conformers of **1**–**3** with those of the heterohelical conformers indicated that the steric bulkiness restricted the conformations of both homohelical and heterohelical isomers (Fig. 5b and c). The restriction of conformations can be the prerequisite for the cooperative helicity induction, since the interactions between the two ZnBL units occurs with defined relative orientations of two helices. The more favorable conformational energy of homohelical **3** than heterohelical **3** cannot be reproduced by the modeling studies since the origin of the energy difference could be dispersion forces and more elaborate calculations such as those with the MP2 theory may be needed.

More detailed molecular modeling was carried out for **3**. The grid search for two bond rotations around O19–C1 and

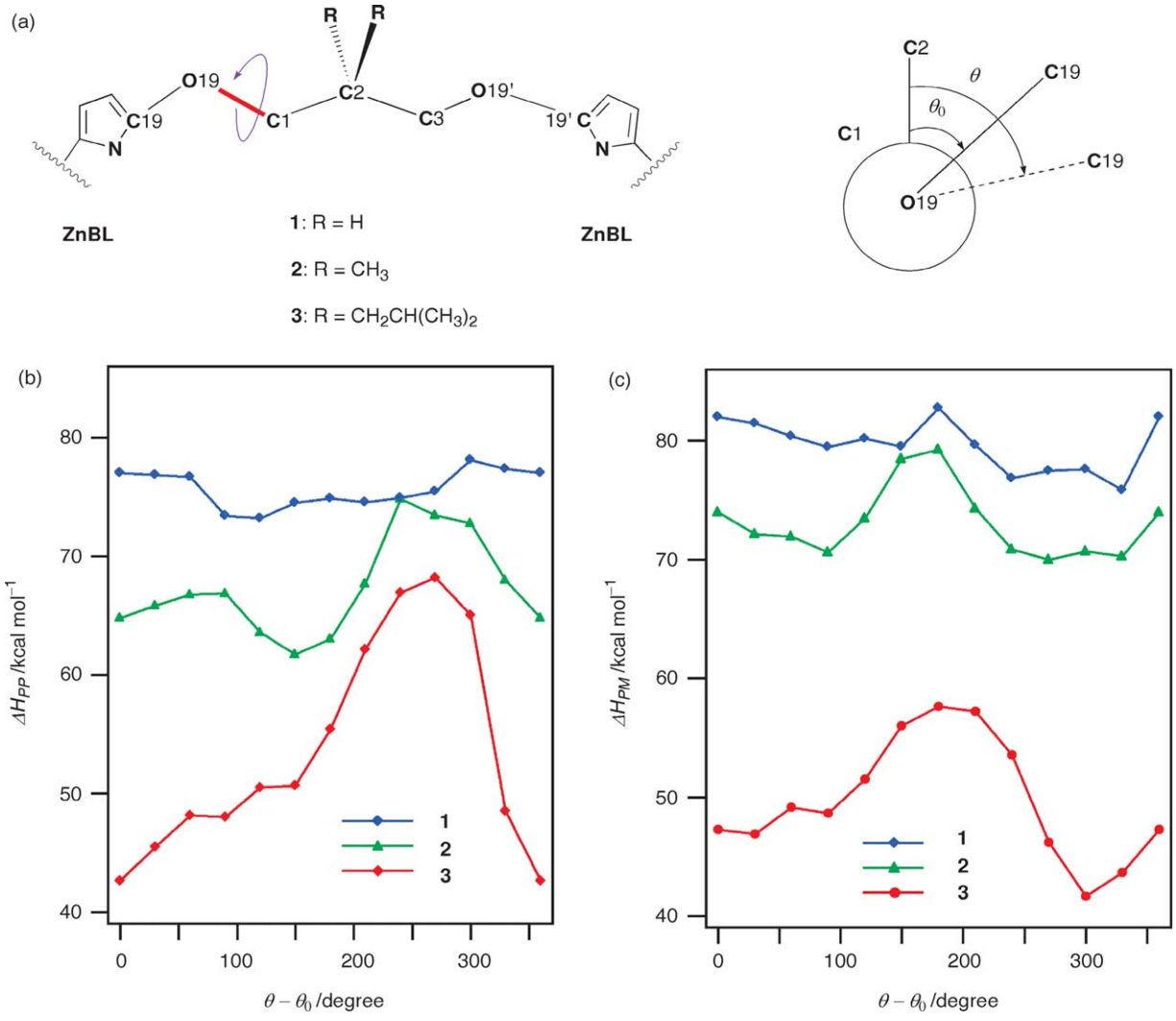

Figure 5. (a) A conceptual representation of the grid search for the ZnBL dimers, (b) potential energies of homohelical (*PP*) conformers and (c) those of heterohelical (*PM*) conformers of **1**–**3** obtained by the grid search calculations (MOPAC PM3).

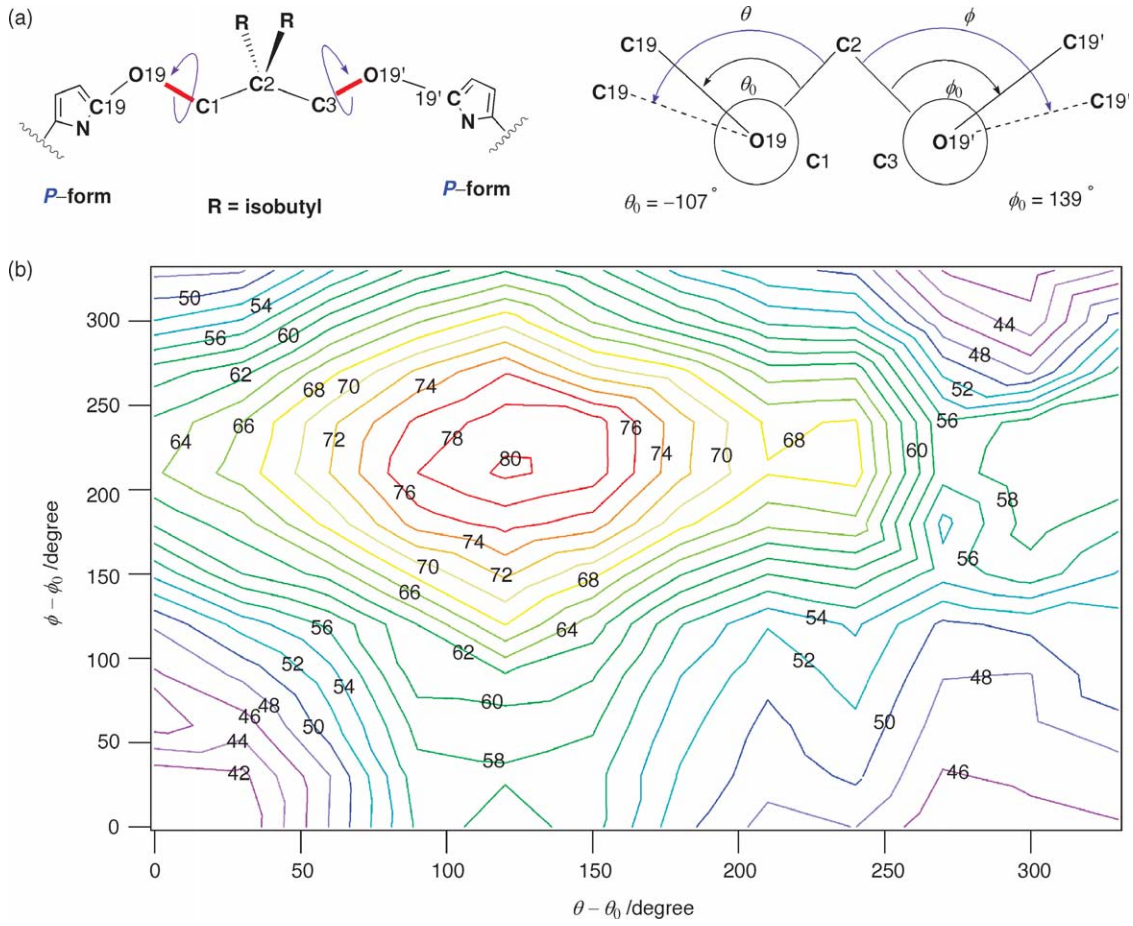

Figure 6. (a) A definition of two degrees of rotation, (b) the contour map of ΔH_{PP} (kcal/mol) for ZnBL dimer **3** as a function of dihedral angles $\theta-\theta_0$ and $\phi-\phi_0$.

C3–O19′ represented by $\theta-\theta_0$ and $\phi-\phi_0$, respectively, was examined as shown in Figure 6a. The conformational optimization for the *PP* form was performed using the MOPAC PM3 method for 144 pairs of $\theta-\theta_0$ and $\phi-\phi_0$ at 30° intervals. The contour map for ΔH_{PP} is shown in Figure 6b, where the contour lines are drawn at 2 kcal/mol intervals. Two most stable conformers were obtained in two sets of ($\theta-\theta_0$, $\phi-\phi_0$): (0, 0) and (300, 330) yielded $\Delta H_{PP}=39.00$ kcal/mol (structure in Fig. 7a) and 41.19 kcal/mol (structure in Fig. 7b), respectively. In both of the structures, proximity between the 18-methyl group in one ZnBL subunit and the A-ring in the other ZnBL was found, indicating that van der Waals interaction between the two ZnBL subunits contributed to the stabilization of the homohelical conformers.

In ^{1}H NMR spectra, upfield shifts of the 18-Me signals of the ZnBL subunits in the homohelical conformers of **2** and **3** were observed in comparison with the 18-Me signal of the monomer **4** (Fig. 8, $\Delta\delta$; −0.185 and −0.365 ppm for **2** and

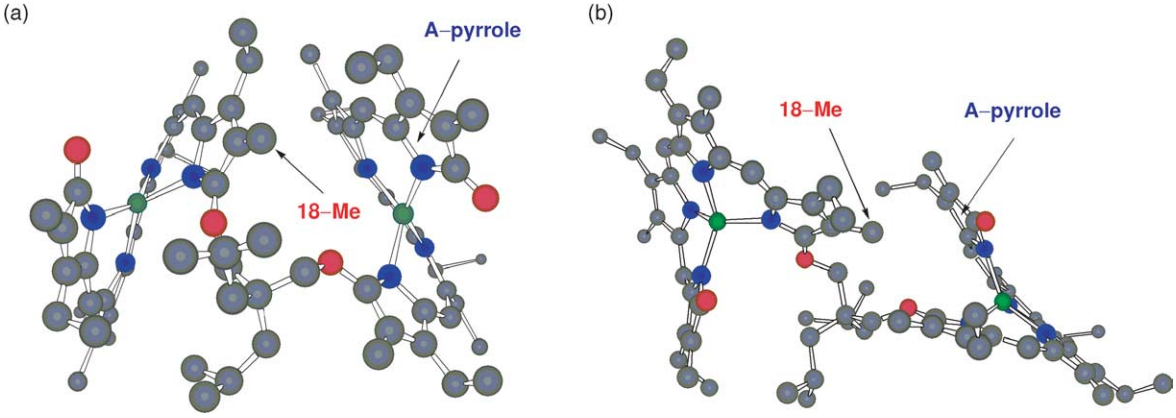

Figure 7. The most stable homohelical structures for **3** obtained from the contour map in Figure 6b. Hydrogen atoms are omitted for clarify; (a) ($\theta-\theta_0$, $\phi-\phi_0$)=(0, 0), (b) ($\theta-\theta_0$, $\phi-\phi_0$)=(300, 330).

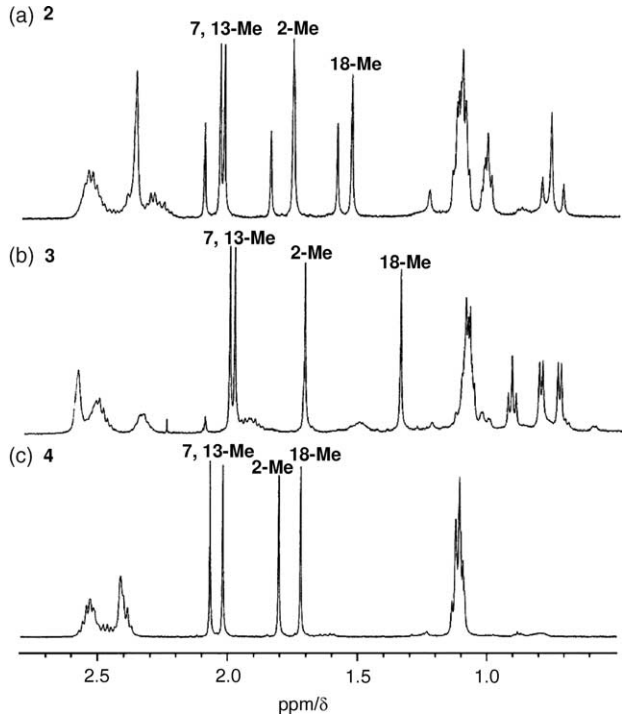

Figure 8. The expanded region of ^{1}H NMR spectra of (a) **2** (1.09 mM), (b) **3** (1.09 mM), and (c) **4** (2.17 mM). These spectra were obtained in $CDCl_3$ at 223 K. The 2-, 7-, 13-, and 18-methyls of the homohelical conformers are noted in the spectra.

3, respectively) showing that the 18-methyl groups in the homohelical conformers of **2** and **3** were magnetically affected by the ZnBL's π-conjugation system. That is, the upfield shifts of the 18-Me signals in the homohelical conformers agreed with the proximity of the 18-Me to the A-pyrrole ring of the neighboring subunit. According to the modeling study, the shortest distances between the 18-methyl hydrogen (18-H) and the A-ring pyrrole carbon (2-C or 4-C) in the homohelical conformer of **3** were 3.54 Å (18-H–4-C in the most stable conformer) and 3.37 Å (18-H–2-C in the next most stable conformer), while those in the heterohelical conformer were 4.51 Å (18-H–4-C in the most stable conformer) and 7.45 Å (18-H–2-C in the next most stable conformer). Thus, the homohelical conformer takes a folded conformation, where the methyl group is in van der Waals contact with the pyrrole ring. The NMR and modeling study revealed that introduction of the bulky substituents on the spacer should lead to conformational restriction in **2** and **3** to facilitate effective interactions between the ZnBL subunits stabilizing the homohelical structures.[21] The upfield shift was more remarkable in **3** than in **2**, and thus, the inter-subunit interaction stabilizing the homohelical structures should be more effective in **3**.

2.4. Homohelicity induction in ZnBL dimers upon complexation with chiral guests

Homohelicity induction in **1**–**3** upon complexation with chiral amine and α-amino esters was examined using CD spectroscopy. As reported previously,[10] complexation of chiral amines and α-amino esters to ZnBL gives rise to generation of alternative Cotton effects in the high (ca. 400 nm) and low energy (ca. 800 nm) regions, and the CD intensity in the high energy region is linearly proportional to the helicity excess (h.e.) of ZnBL. In the case of ZnBL dimer systems, h.e. is represented by Eq. 1

$$\text{h.e. } (\%) = \frac{[MM]-[PP]}{[MM]+[PP]+[PM]} \times 100 \qquad (1)$$

where [*PP*], [*MM*], and [*PM*] are concentrations of *PP*, *MM*, and *PM* conformers, respectively. According to this equation, the high h.e. value in the ZnBL dimer–guest complex system refers to effective homohelicity induction, and thus, the CD intensity induced by complexation with chiral guests is a good index for homohelicity induction. In Fig. 9 are shown CD spectra in the high-energy region for the ZnBL dimers **1**–**3** and the monomer **4** in $CHCl_3$ at 223 K in the presence of (*R*)-1-(1-naphthyl)ethylamine ((*R*)-NEA). The values of Δε were normalized by a molar concentration of the ZnBL subunit. To achieve complexation of the amine to each ZnBL subunit, addition of an excess amount of the guest as well as low-temperature experiments were required. Although a positive sign indicating *M*-helicity induction[10,22] was observed for each dimer, the intensity varied in the spacer: compared to the monomer **4**, the dimers **2** and **3** showed larger CD intensities, indicating that the cooperative motion to adopt *MM* homohelicity was allowed between the ZnBL subunits. On the other hand, the dimer **1** exhibited less effective CD induction, indicating negative cooperativity of the ZnBL subunits in homohelicity induction. The CD data obtained for a series of chiral guests are summarized in Table 1. For each guest, the predominant helicity of ZnBL in **1**–**3** induced by the complexation was the same as that in **4**, and the CD intensity increased in the order of **1**<**4**<**2**<**3**. Thus, the preorganization of the *PP* and *MM* homohelical conformers plays a substantial role in helicity–helicity synchronization of the ZnBL subunits triggered by point chirality–helicity interaction between the ZnBL subunit and the chiral guest. As discussed above, the preorganization effect was more remarkable in **3** than in **2**, and the large cooperativity in homohelicity induction should owe to the inter-subunit interactions optimized by the preorganization.

^{1}H NMR experiments afforded further information about the complexation-induced homohelicity induction: the quantitative analyses were allowed by analyzing magnetically distinguishable ^{1}H NMR signals of the *PP*, *MM* and *PM*

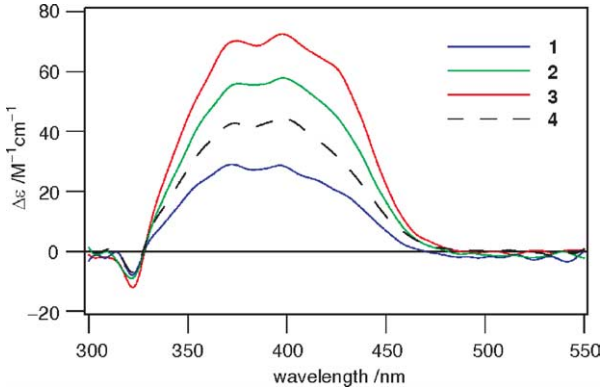

Figure 9. CD spectra in the high-energy region for **1**–**4** in the presence of (*R*)-NEA in $CHCl_3$ at 223 K: [ZnBL subunit]=40.4–43.1 μM, [(*R*)-NEA]=0.0530–0.0544 M.

Table 1. The differential dichroic absorption ($\Delta\varepsilon$)[a] and helicity excesses (h.e.s)[b] for the complexes of **1**–**4** with chiral amine and α-amino esters

Compound	$\Delta\varepsilon$ (M^{-1} cm^{-1}) (λ (nm), helicity[c]), h.e. (%)				
	(*R*)-NEA[d]	L-Leu-OMe[d]	D-PhGly-OMe[d]	L-Phe-OMe[d]	L-Asp-$(OMe)_2$[d]
1	26.6 (397, *M*), 34	33.2 (402, *M*), 40	−36.3 (399, *P*), 34	47.9 (398, *M*), 46	60.1 (404, *M*), 66
2	57.9 (398, *M*), 50	66.1 (398, *M*), 65	−69.9 (401, *P*), 68	85.8 (397, *M*), 74	97.7 (404, *M*), 85
3	72.5 (398, *M*), 68	90.4 (402, *M*), 76	−91.7 (403, *P*), 78	101.8 (398, *M*), 86	114.5 (402, *M*), 94
4	44.2 (397, *M*), 35	53.8 (401, *M*), 55	−61.2 (403, *P*), 54	75.2 (400, *M*), 67	89.2 (404, *M*), 84

[a] The values of $\Delta\varepsilon$ were corrected by a ZnBL unit. The spectral data were taken in $CHCl_3$ at 223 K.
[b] Determined by ^{1}H NMR spectra in $CDCl_3$ at 223 K.
[c] Helicity predominantly formed.
[d] Abbreviations: NEA, 1-(1-naphthyl)ethylamine; Leu-OMe, leucine methyl ester; PhGly-OMe, α-phenylglycine methyl ester; Phe-OMe, phenylalanine methyl ester; Asp-$(OMe)_2$, aspartic acid dimethyl ester.

conformers. In Figure 10 are shown ^{1}H NMR spectra of **2** in $CDCl_3$ at 223 K in the absence and presence of (*R*)-NEA. Upon addition of increasing amounts of (*R*)-NEA, each signal exhibited splitting, and the chemical shift change reached a plateau in the presence of an excess amount of (*R*)-NEA, indicating that full complexation of the ZnBL subunits with the guest molecules was achieved.[23] The major set of the signals split into two with the different integral ratios, whereas the minor into two with the same ratios. As complexation with chiral guests gives rise to identical and diastereomeric relationships of the ZnBL frameworks in the homohelical and heterohelical dimers, respectively, the former and latter splitting behaviors were due to formation of the homohelical and heterohelical **2**·2NEA, respectively. Thus, comparison of the integral ratios of the three conformers (complexed *PP*-, *MM*-, and *PM*-conformers) allowed us to determine the ratio of *PP*-**2**·2NEA: *PM*-**2**·2NEA: *MM*-**2**·2NEA as 16:18:66. In **1** and **3**, the distinguishable signal sets also afforded the distribution of the three conformers; 3:60:37 and 16:0:84 for **1** and **3**, respectively. For the other guests, the ratios of the conformers in **1**–**3** were similarly determined, and the h.e.s were obtained according to Eq. 1, as summarized in Table 1. Interesting is that no *PM*-conformer was observed for **3** on ^{1}H NMR upon complexation with any guests (see Table 3 in Section 4). Especially, in the case of the **3**·2Asp-$(OMe)_2$ complex, the homohelicity conformer was exclusively formed (h.e., 94%). In all dimers, the h.e.s increased in the order of NEA < Leu-OMe < PhGly-OMe < Phe-OMe < Asp-$(OMe)_2$. This tendency was similar to that of the monomer **4**. In addition, the helicity predominantly formed was determined by the point chirality of the chiral guests. That is, chiral molecular recognition between the ZnBL framework and the chiral guests was essential to determination of thermodynamic stability of each chiral helical ZnBL subunit complexed with the chiral guest. On the other hand, as indicated in the ^{1}H NMR as well as CD spectra, the h.e.s of **2** and **3** were larger than those of **4** for all guests employed in the present study, clearly showing positive cooperativity in homohelicity induction. Obviously, the h.e. increased with the increase in the bulkiness of the substituents on the spacer. Therefore, the inter-subunit interaction, afforded by the appropriate spacers, is essential to the helicity amplification, that is, the cooperative homohelicity induction.

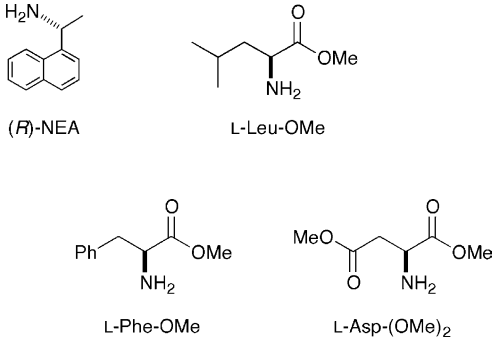

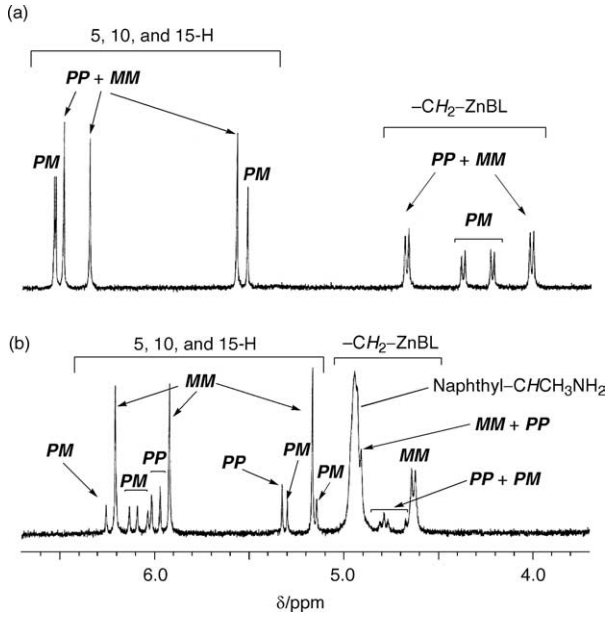

Figure 10. The expanded region of ^{1}H NMR spectra of **2** (1.09 mM) in $CDCl_3$ at 223 K; (a) **2** and (b) **2** and (*R*)-NEA (6.53 mM).

It is a common feature among **1**–**3** that the increase in the h.e. gives rise to the increase in the CD intensity, and as shown in Figure 11, these two are validly proportional to each other. The slopes for **1**–**4** are almost the same (Table 2). Thus, in each dimer, the CD signal and intensity reflect the absolute structures of the guest amine and α-amino esters. The structural information of the guests are amplified most effectively by **3**, compared to **4**, and such chiral signal amplification should not be achieved without steric interactions inducing the chiral homohelical framework.

3. Conclusions

We investigated homohelicity induction in the propylene-linked ZnBL dimers **1**–**3** in which the substituents

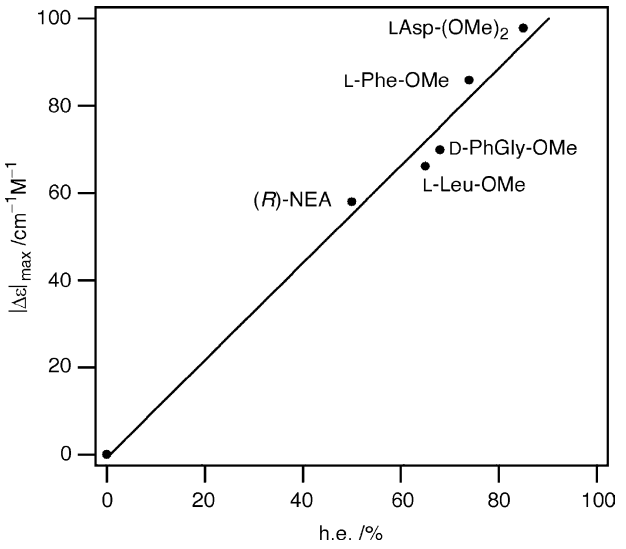

Figure 11. The linear correlation of h.e. and $\Delta\varepsilon$ in the complexes of **2** with various chiral guests. The h.e. and $\Delta\varepsilon$ were determined by ^{1}H NMR spectroscopy and CD spectra, respectively.

Table 2. The slopes (α) and correlation coefficients (R) of the plots of $\Delta\varepsilon$ versus h.e. for **1**–**4**

Compound	α	R
1	0.93	0.93
2	1.11	0.95
3	1.18	0.96
4	1.09	0.96

introduced onto the central carbon of the spacer varied in bulkiness. Introduction of methyls and isobutyls led to preorganization of the homohelical conformers *PP* and *MM*. Such a preorganization effect played an essential role in cooperative homohelicity induction triggered by chiral recognition of the ZnBL subunit for guests such as chiral amine and α-amino esters. The increase in bulkiness of the substituents on the spacer gave rise to enhancement of positive cooperativity in homohelicity induction of the ZnBL dimer by complexation with the chiral guests. Especially, the homohelicity induction in **3** was significantly enhanced, and the *MM*-homohelical conformer was exclusively formed upon complexation with L-Asp-(OMe)$_2$ (h.e., 94%). The results obtained in the present study show that this concept is potentially applicable to design of molecular sensors that can amplify signals for analytes.

4. Experimental

4.1. General

^{1}H NMR spectra were obtained on a Jeol JNM-LA400 (400 MHz) or a Jeol JNM GA500 (500 MHz) FT-NMR spectrometer, and the chemical shifts are reported in parts per million (ppm) downfield from TMS (0 ppm) as an internal standard. Elemental analyses were recorded on a Yanaco CHN-CORDER MT3 recorder. FAB MS spectra were obtained on a Finnigan Mat TSQ-70 spectrometer, using 3-nitrobenzyl alcohol as a matrix. Infrared absorption spectra were obtained on a Shimadzu FTIR-8400S spectrometer as KBr pellets. Melting points were determined with a Yanako MP-500D. Gel permeation chromatography was performed using SHODEX GPC K-2001 and K-2002 poly(styrene) gel column packages connected successively, where CH_2Cl_2 was used as eluent. UV–vis absorption spectra were obtained on a Shimadzu UV-3100 spectrometer. Circular dichroism (CD) spectra at 223 K were recorded on a Jasco J-600 spectrometer equipped with an Oxford DN1704 cryostat. The sample solutions for UV–vis and CD spectral analyses were prepared in a volumetric flask at 288 K, and the concentrations at 223 K were corrected on the basis of the thermal expansion coefficient of $CHCl_3$ (0.00126 K^{-1}).

4.2. Materials and solvents

Preparation of zinc bilinone **1** was reported previously.[8] α-Amino esters for the spectroscopic measurements were obtained by neutralization of the commercially available hydrochlorides followed by distillation just prior to use: L-Phe-OMe·HCl and L-Asp-(OMe)$_2$·HCl were purchased from Sigma Chemical Company, L-Leu-OMe·HCl was from Nakalai Tesque, Inc., and D-PhGly-OMe·HCl was from Wako Pure Chemicals Industries. (*R*)-NEA was purchased from Tokyo Chemical Industries and used after distillation. All solvents for the UV–vis, CD, and NMR measurements were of spectroscopic grade.

4.3. Experimental procedures

4.3.1. 19,19′-(2,2-Dimethyl-1,3-propylenedioxy)di-(3,8,12,17-tetraethyl-1,21-dihydro-2,7,13,18-tetramethyl-22*H*-bilin-1-one) (5). A mixture of 2,2-dimethyl-1,3-propanediol **7** (11.8 mg, 0.113 mmol) and sodium hydride (60% oil dispersion, 18.0 mg, 0.450 mmol) in dry THF (6 mL) was stirred at rt for 1 h under N_2. The (5-oxoniaporphynato)zinc(II) chloride **9** (131 mg, 0.226 mmol) was added, and the mixture was stirred at rt for 24 h. The solvent was removed on a rotary evaporator, and CH_2Cl_2 (50 mL) was added to the residue. The solution was washed with satd NH_4Cl (50 mL). The organic layer was vigorously shaken with a phthalate buffer solution (pH =4.0, 50 mL×3), washed with water (50 mL) and satd brine (50 mL), and then, dried over anhydrous Na_2SO_4. The solvent was removed by evaporation, and the residue was purified by silica gel column chromatography (dichloromethane/benzene/acetone = 7.5:7.5:1, v/v/v, as eluent). Further purification by gel permeation chromatography on HPLC followed by reprecipitation from CH_2Cl_2–hexane afforded **5** as a dark blue solid (42.5 mg, 0.0399 mmol, 35%): mp>250 °C (dec) ^{1}H NMR (400 MHz, $CDCl_3$) δ 0.69 (s, 6H, $(CH_3)_2C(CH_2O–)_2$), 1.05–1.16 (m, 24H, $CH_3CH_2–$), 1.60 (s, 6H, $CH_3–$), 1.77 (s, 6H, $CH_3–$), 1.90 (s, 6H, $CH_3–$), 2.11 (s, 6H, $CH_3–$), 2.33–2.41 (m, 8H, $CH_3CH_2–$), 2.49–2.61 (m, 8H, $CH_3CH_2–$), 4.05 (br s, 4H, $–CH_2O–$), 5.69 (s, 2H, *meso*-H), 6.23 (s, 2H, *meso*-H), 6.62 (s, 2H, *meso*-H), 10.19 (br s, 2H, NH), 12.65 (br s, 2H, NH); IR (KBr) 2964, 2931, 2867, 1701, 1589, 1215 cm^{-1}; FAB MS *m*/*z* 1064 (M^+). Anal. Calcd for $C_{67}H_{84}N_8O_4\cdot0.5H_2O$: C 74.90, H 7.97, N 10.43. Found: C 74.62, H 8.17, N 10.11.

4.3.2. Zinc complex of 5 (2). To a solution of **5** (36.1 mg, 0.0339 mmol) in CH_2Cl_2 (6 mL) was added a solution of

Table 3. The ratios of the homohelical and heterohelical conformers (*PP*:*PM*:*MM*) for the complexes of ZnBL dimers **1–3** with amines and α-amino esters in $CDCl_3$ at 223 K: [ZnBL subunit] = 2.15–2.19 mM, [guest] = 6.53–10.9 mM

Compound	*PP*:*PM*:*MM*					
	Benzylamine	(*R*)-NEA	L-Leu-OMe	D-PhGly-OMe	L-Phe-OMe	L-Asp-$(OMe)_2$
1	15:70:15	3:60:37	3:54:43	38:57:5	6:42:52	4:26:70
2	39:22:39	16:18:66	9:27:74	75:18:7	6:14:80	5:5:90
3	49:2:49	16:0:84	12:0:88	89:0:11	7:0:93	3:0:97

zinc acetate (74.0 mg, 0.337 mmol) in methanol (3 mL), and then, the mixture was stirred at rt for 1 h. The solvent was removed on a rotary evaporator, and the residue was dissolved in CH_2Cl_2 (25 mL) and washed with water (20 mL×2). The organic layer was dried over anhydrous Na_2SO_4, and the solvent was removed by evaporation to afford **2** as a dark green solid (37.4 mg, 0.0314 mmol, 93%). Further purification was not performed because demetallation of Zn(II) might occurred: mp 178–180 °C (dec) ^{1}H NMR (400 MHz, $CDCl_3$) δ 0.73 (s, 3H for *PM*, $(CH_3)_2C(CH_2O–)_2$), 0.81 (s, 6H for *PP*+*MM*, $(CH_3)_2C(CH_2O–)_2$), 1.25 (s, 3H for *PM*, $(CH_3)_2C(CH_2O–)_2$), 1.00–1.18 (m, 24H for *PP*+*MM* and 24H for *PM*, $CH_3CH_2–$), 1.50 (s, 6H for *PP*+*MM*, $CH_3–$), 1.60 (s, 6H for *PM*, $CH_3–$), 1.73 (s, 6H for *PP*+*MM* and 6H for *PM*, $CH_3–$), 1.81 (s, 6H for *PM*, $CH_3–$), 1.98 (s, 6H for *PP*+*MM*, $CH_3–$), 2.02 (s, 6H for *PP*+*MM*, $CH_3–$), 2.08 (s, 6H for *PM*, $CH_3–$), 2.21–2.57 (m, 16H for *PP*+*MM* and 16H *PM*, $CH_3CH_2–$), 3.93–3.95 (d, *J*=10.0 Hz, 2H for *PP*+*MM*, $–CH_2O–$), 4.22–4.24 (d, *J*=10.0 Hz, 2H for *PM*, $–CH_2O–$), 4.36–4.38 (d, *J*=10.0 Hz, 2H for *PM*, $–CH_2O–$), 4.73–4.76 (d, *J*=10.0 Hz, 2H for *PP*+*MM*, $–CH_2O–$), 5.46 (s, 2H for *PP*+*MM*, *meso*-H), 5.50 (s, 2H for *PM*, *meso*-H), 6.30 (s, 2H for *PP*+*MM*, *meso*-H), 6.46 (s, 2H for *PP*+*MM*, *meso*-H), 6.52 (s, 2H for *PM*, *meso*-H), 6.53 (s, 2H for *PM*, *meso*-H); IR (KBr) 2964, 2929, 2869, 1652, 1573, 1207 cm^{-1}; FAB MS *m*/*z* 1188 (M^+). Anal. Calcd for $C_{67}H_{80}N_8O_4Zn_2\cdot H_2O$: C 66.50, H 6.83, N 9.26. Found: C 66.54, H 6.86, N 9.17.

4.3.3. 19,19′-(2,2-Diisobutyl-1,3-propylenedioxy)di-(3,8,12,17-tetraethyl-1,21-dihydro-2,7,13,18-tetramethyl-22*H*-bilin-1-one) (6). According to a similar procedure to the preparation of **5**, the reaction of a mixture of 2,2-diisobuthyl-1,3-propanediol **8** (22.8 mg, 0.121 mmol) and sodium hydride (60% oil dispersion, 27.8 mg, 0.695 mmol) in dry THF (6 mL) with **9** (141 mg, 0.243 mmol) afforded **6** as a dark blue solid (42.6 mg, 0.0371 mmol, 31%): mp 268–270 °C (dec) ^{1}H NMR (400 MHz, $CDCl_3$) δ 0.72–0.74 (d, 12H, *J*=6.3 Hz, $(CH_3)_2CHCH_2–$), 0.98 (t, 6H, *J*=7.8 Hz, $CH_3CH_2–$), 1.03–1.04 (d, 4H, *J*=4.8 Hz, $(CH_3)_2CHCH_2–$), 1.09–1.16 (m, 18H, $CH_3CH_2–$), 1.41–1.54 (m, 6H for $CH_3–$ and 2H for $(CH_3)_2CHCH_2–$), 1.75 (s, 6H for $CH_3–$), 1.97 (s, 6H for $CH_3–$), 2.06–2.12 (m, 6H for $CH_3–$ and 4H for $CH_3CH_2–$), 2.36–2.42 (q, 4H, *J*=7.3 Hz, $CH_3CH_2–$), 2.49–2.59 (m, 8H, $CH_3CH_2–$), 3.58–4.81 (br, 4H, $–CH_2O–$), 5.69 (s, 2H, *meso*-H), 5.97 (s, 2H, *meso*-H), 6.57 (s, 2H, *meso*-H), 10.33 (br s, 2H, NH), 12.79 (br s, 2H, NH); IR (KBr) 2964, 2929, 2869, 1704, 1558, 1215 cm^{-1}; FAB MS *m*/*z* 1148 (M^+). Anal. Calcd for $C_{73}H_{96}N_8O_4\cdot 0.5H_2O$: C 75.68, H 8.44, N 9.67. Found: C 75.67, H 8.66, N 9.53.

4.3.4. Zinc complex of 6 (3). According to the procedure described for **2**, the reaction of **6** (47.2 mg, 0.0411 mmol) in CH_2Cl_2 (5 mL) with zinc acetate (230 mg, 1.05 mmol) in methanol (3 mL) afforded **3** as a dark green solid (47.4 mg, 0.0371 mmol, 90%): mp 272–274 °C (dec) ^{1}H NMR (400 MHz, $CDCl_3$) δ 0.65–0.66 (d, *J*=6.4 Hz, 6H for *PM*, $(CH_3)_2CHCH_2–$), 0.73–0.75 (m, 6H for *PP*+*MM* and 6H for *PM*, $(CH_3)_2CHCH_2–$), 0.81–0.82 (d, *J*=6.4 Hz, 6H for *PP*+*MM*, $(CH_3)_2CHCH_2–$), 0.95 (t, *J*=7.6 Hz, 6H for *PP*+*MM*, $CH_3CH_2–$), 1.03 (t, *J*=7.6 Hz, 6H for *PM*, $CH_3CH_2–$), 1.06–1.21 (m, 18H for *PP*+*MM* and 24H for *PM*, $CH_3CH_2–$ and 4H for *PP*+*MM* and 4H for *PM*, $(CH_3)_2CHCH_2–$), 1.36 (s, 6H for *PP*+*MM*, $CH_3–$), 1.49–1.59 (m, 2H for *PP*+*MM* and 2H for *PM*, $(CH_3)_2CHCH_2–$ and 6H for *PM*, $CH_3–$), 1.71 (s, 6H for *PP*+*MM*, $CH_3–$), 1.82 (s, 6H for *PM*, $CH_3–$), 1.97 (s, 6H for *PP*+*MM*, $CH_3–$), 2.00 (m, 6H for *PP*+*MM* and 6H for *PM*, $CH_3–$), 2.09 (s, 6H for *PM*, $CH_3–$), 2.28–2.59 (m, 16H for *PP*+*MM* and 16H for *PM*, $CH_3CH_2–$), 3.85–3.87 (d, *J*=10.0 Hz, 2H for *PP*+*MM*, $–CH_2O–$), 4.22–4.24 (d, *J*=10.0 Hz, 2H for *PM*, $–CH_2O–$), 4.53–4.55 (d, *J*=10.0 Hz, 2H for *PM*, $–CH_2O–$), 4.95–4.97 (d, *J*=10.0 Hz, 2H for *PP*+*MM*, $–CH_2O–$), 5.43 (s, 2H for *PP*+*MM*, *meso*-H), 5.48 (s, 2H for *PM*, *meso*-H), 6.12 (s, 2H for *PP*+*MM*, *meso*-H), 6.43 (s, 2H for *PP*+*MM*, *meso*-H), 6.53 (s, 2H for *PM*, *meso*-H), 6.55 (s, 2H for *PM*, *meso*-H); IR (KBr) 2962, 2931, 2869, 1652, 1558, 1207 cm^{-1}; FAB MS *m*/*z* 1272 (M^+). Anal. Calcd for $C_{73}H_{92}N_8O_4Zn_2\cdot H_2O$: C 67.74, H 7.32, N 8.66. Found: C 67.68, H 7.37, N 8.65.

4.4. Determination of the distribution of the homohelical and heterohelical conformers

The distribution of the homohelical and heterohelical conformers was determined by comparison of the integral ratios of their ^{1}H NMR signals with one another. The signals assigned to 5-, 10-, 15-Hs or methylene's protons of the spacer ($–OCH_2–$) were monitored in $CDCl_3$ at 223 K. The ratios of the *PP*, *PM* and *MM* conformers for all guests are summarized in Table 3.

References and notes

1. (a) Monod, J.; Wyman, J.; Changeux, J.-P. *J. Mol. Biol.* **1965**, *12*, 88–118. (b) Koshland, D. E., Jr.; Némethy, G.; Filmer, D. *Biochemistry* **1966**, *5*, 365–385. (c) Schachman, H. K. *J. Biol. Chem.* **1988**, *263*, 18583–18586.
2. (a) Monod, J.; Changeux, J.-P.; Jacob, F. *J. Mol. Biol.* **1963**, *6*, 306–329. (b) Perutz, M. F. *Annu. Rev. Biochem.* **1979**, *48*,

327–386. (c) Perutz, M. F.; Fermi, G.; Luisi, B.; Shaanan, B.; Liddington, R. C. *Acc. Chem. Res.* **1987**, *20*, 309–321.
3. (a) Piguet, C.; Bernardinelli, G.; Hopfgartner, G. *Chem. Rev.* **1997**, *97*, 2005–2062. (b) Ziegler, M.; von Zelewsky, A. *Coord. Chem. Rev.* **1998**, *177*, 257–300. (c) McQuade, D. T.; Pullen, A. E.; Swager, T. M. *Chem. Rev.* **2000**, *100*, 2537–2574. (d) Hill, D. J.; Mio, M. J.; Prince, R. B.; Hughes, T. S.; Moore, J. S. *Chem. Rev.* **2001**, *101*, 3893–4011. (e) Nakano, T.; Okamoto, Y. *Chem. Rev.* **2001**, *101*, 4013–4038. (f) Yashima, E.; Maeda, K.; Nishimura, T. *Chem. Eur. J.* **2004**, *10*, 42–51.
4. (a) Beer, P. D. *Chem. Soc. Rev.* **1989**, *18*, 409–450. (b) Shinkai, S.; Ikeda, M.; Sugasaki, A.; Takeuchi, M. *Acc. Chem. Res.* **2001**, *34*, 494–503. (c) Takeuchi, M.; Ikeda, M.; Sugasaki, A.; Shinkai, S. *Acc. Chem. Res.* **2001**, *34*, 865–873. (d) Kovbasyuk, L.; Kraemer, R. *Chem. Rev.* **2004**, *104*, 3161–3187.
5. (a) Takeuchi, M.; Imada, T.; Shinkai, S. *Angew. Chem., Int. Ed.* **1998**, *37*, 2096–2099. (b) Ayabe, M.; Ikeda, A.; Kubo, Y.; Takeuchi, M.; Shinkai, S. *Angew. Chem., Int. Ed.* **2002**, *41*, 2790–2792. (c) Raker, J.; Glass, T. E. *J. Org. Chem.* **2002**, *67*, 6113–6116. (d) Sessler, J. L.; Maeda, H.; Mizuno, T.; Lynch, V. M.; Furuta, H. *J. Am. Chem. Soc.* **2002**, *124*, 13474–13479. (e) Chang, S.-U.; Um, M.-C.; Uh, H.; Jang, H.-Y.; Jeong, K.-S. *Chem. Commun.* **2003**, 2026–2027. (f) Thordarson, P.; Bijsterveld, E. J. A.; Elemans, J. A. A. W.; Kasak, P.; Nolte, R. J. M.; Rowan, A. E. *J. Am. Chem. Soc.* **2003**, *125*, 1186–1187. (g) Kawai, H.; Katoono, R.; Nishimura, K.; Matsuda, S.; Fujiwara, K.; Tsuji, T.; Suzuki, T. *J. Am. Chem. Soc.* **2004**, *126*, 5034–5035. (h) Chang, S.-Y.; Jang, H.-Y.; Jeong, K.-S. *Chem. Eur. J.* **2004**, *10*, 4358–4366. (i) Gianneschi, N. C.; Nguyen, S. T.; Mirkin, C. A. *J. Am. Chem. Soc.* **2005**, *127*, 1644–1645. (j) Nabeshima, T.; Saiki, T.; Iwabuchi, T.; Akine, S. *J. Am. Chem. Soc.* **2005**, *127*, 5507–5511.
6. (a) Yashima, E.; Matsushima, T.; Okamoto, Y. *J. Am. Chem. Soc.* **1997**, *119*, 6345–6359. (b) Wilson, A. J.; Masuda, M.; Sijbesma, R. P.; Meijer, E. W. *Angew. Chem., Int. Ed.* **2005**, *44*, 2275–2279.
7. (a) Mizuno, T.; Aida, T. *Chem. Commun.* **2003**, 20–21. (b) Li, W.-S.; Jiang, D.-L.; Suna, Y.; Aida, T. *J. Am. Chem. Soc.* **2005**, *127*, 7700–7702.
8. Mizutani, T.; Sakai, N.; Yagi, S.; Takagishi, T.; Kitagawa, S.; Ogoshi, H. *J. Am. Chem. Soc.* **2000**, *122*, 748–749.
9. Hamakubo, K.; Yagi, S.; Nakazumi, H.; Mizutani, T.; Kitagwa, S. *Tetrahedron Lett.* **2005**, *46*, 7151–7154.
10. (a) Mizutani, T.; Yagi, S.; Honmaru, A.; Ogoshi, H. *J. Am. Chem. Soc.* **1996**, *118*, 5318–5319. (b) Mizutani, T.; Yagi, S.; Honmaru, A.; Murakami, S.; Furusyo, M.; Takagishi, T.; Kitagawa, S.; Ogoshi, H. *J. Org. Chem.* **1998**, *63*, 8769–8784.
11. (a) Führhop, J.-H.; Salek, A.; Subramanian, J.; Mengersen, C.; Besecke, S. *Liebigs Ann. Chem.* **1975**, 1131–1147. (b) Führhop, J.-H.; Kruger, P.; Sheldrick, W. S. *Liebigs Ann. Chem.* **1977**, 339–359.
12. Führhop, J.-H.; Kruger, P. *Liebigs Ann. Chem.* **1977**, 360–370.
13. For examples, of molecular orbital studies of host–guest binding, see (a) Meyer, E. A.; Castellano, R. K.; Diederich, F. *Angew. Chem., Int. Ed.* **2003**, *42*, 1210–1250. (b) Dos Santos, H. F.; Duarte, H. A.; Sinisterra, R. D.; De Melo Mattos, S. V.; De Oliveira, L. F. C.; De Almeida, W. B. *Chem. Phys. Lett.* **2000**, *319*, 569–575. (c) Takahashi, O.; Kohno, Y.; Iwasaki, S.; Saito, K.; Iwaoka, M.; Tomoda, S.; Umezawa, Y.; Tsuboyama, S.; Nishio, M. *Bull. Chem. Soc. Jpn.* **2001**, *74*, 2421–2430. (d) Schneider, H.-J.; Yatsimirsky, A. *Principles and Methods in Supramolecular Chemistry*; Wiley: Chichester, 2000. (e) Hunter, C. A.; Sanders, J. K. M. *J. Am. Chem. Soc.* **1990**, *112*, 5525–5534.
14. Iwata, S.; Morokuma, K. *J. Am. Chem. Soc.* **1973**, *95*, 7563–7575.
15. Ruangpornvisuti, V. *THEOCHEM* **2004**, *686*, 47–55.
16. Venayagamoorthy, M.; Ford, T. A. *J. Mol. Struct.* **2001**, *565–566*, 399–409.
17. Fernandez-Alonso, M. d. C.; Canada, F. J.; Jimenez-Barbero, J.; Cuevas, G. *J. Am. Chem. Soc.* **2005**, *127*, 7379–7386.
18. Mizutani, T.; Ema, T.; Ogoshi, H. *Tetrahedron* **1995**, *51*, 473–484.
19. The initial structures of **1**–**3** were generated by geometrical optimizaton performed by molecular mechanics calculations (MMFF94 force field) followed by semi-empirical molecular orbital calculations (MOPAC PM3 level), using a *Spartan '02* program package; Wavefunction, Inc., Irvine, California.
20. The molecular modelling was performed at the MOPAC PM3 level using the *winMOPAC 3.5 professional* program package; Fujitsu Co., Chiba, Japan.
21. Inter-subunit interactions to stabilize the homohelicity structure was also found in the homohelical ZnBL dimer with a chiral cyclohexane-1,2-dioxy spacer: see, Yagi, S.; Sakai, N.; Yamada, R.; Takahashi, H.; Mizutani, T.; Takagishi, T.; Kitagawa, S.; Ogoshi, H. *Chem. Commun.* **1999**, 911–912.
22. (a) Krois, D.; Lehner, H. *J. Chem. Soc., Perkin Trans. 2* **1989**, 2085–2091. (b) Krois, D.; Lehner, H. *J. Chem. Soc., Perkin Trans. 1* **1989**, 2179–2185. (c) Krois, D.; Lehner, H. *J. Chem. Soc., Perkin Trans. 2* **1993**, 1351–1360.
23. Upon addition of the guest, an averaged spectrum of complexed and uncomplexed dimers was observed for each conformer, and the three conformers were independently observed even upon complexation with the guest. Thus, the complexation–dissociation between the dimer and the guest was faster than the ^{1}H NMR time scale under the present conditions, whereas the interconversion among the three conformers was slower.